



VuLCAN : A Low-cost, Low-power Embedded Visible Light Communication And Networking Platform

Artem Ageev, Emiliano Luci, Chiara Petrioli, Nupur Thakker*

Computer Science Department
University of Rome “La Sapienza”
Rome, Italy
[petrioli,thakker]@di.uniroma1.it

ABSTRACT

Visible Light Communication (VLC) offers a key alternative to the spectrum-challenged Radio Frequency (RF)-based forms of data transmission by tapping an unutilized and unregulated frequency band. Carefully designed low-cost VLC devices have the potential to enable the Internet of Things (IoT) at scale by reducing the current RF spectrum congestion, which is one of the major obstacles to the pervasiveness of the IoT. Wide adoption of VLC devices is however hindered by their current shortcomings, including low data rate, very short range and inability to communicate in noisy environment. In this paper we describe a new software-defined VLC prototype named VuLCAN for Visible Light Communication And Networking that overcomes these limitations. VuLCAN is based on an ARM Cortex M7 core microcontroller with fast sampling analog-to-digital converter along with power-optimized Digital Signal Processing (DSP) libraries. Using BFSK modulation, the prototype achieves a data rate of 65 Kbps over a communication range of 4.5 m. VuLCAN also provides robust and reliable communications in highly illuminated environments (up to 800 lux) using only a low power Light Emitting Diode (LED), largely exceeding the capabilities of current state-of-the-art prototypes.

CCS CONCEPTS

- **Hardware → Emerging optical and photonic technologies;**
- **Computer systems organization → Embedded hardware; Embedded software.**

KEYWORDS

Visible light communication; free-space optical; internet of things; embedded software

ACM Reference Format:

Artem Ageev, Emiliano Luci, Chiara Petrioli, Nupur Thakker. 2019. VuLCAN : A Low-cost, Low-power Embedded Visible Light Communication And Networking Platform. In *22nd Int'l ACM Conference on Modeling, Analysis and Simulation of Wireless and Mobile Systems (MSWiM '19)*, November

* Author names are listed in alphabetical order, which is not indicative of contribution.

Permission to make digital or hard copies of all or part of this work for personal or classroom use is granted without fee provided that copies are not made or distributed for profit or commercial advantage and that copies bear this notice and the full citation on the first page. Copyrights for components of this work owned by others than ACM must be honored. Abstracting with credit is permitted. To copy otherwise, or republish, to post on servers or to redistribute to lists, requires prior specific permission and/or a fee. Request permissions from permissions@acm.org.

MSWiM '19, November 25–29, 2019, Miami Beach, FL, USA

© 2019 Association for Computing Machinery.

ACM ISBN 978-1-4503-6904-6/19/11...\$15.00

<https://doi.org/10.1145/3345768.3355919>

25–29, 2019, Miami Beach, FL, USA. ACM, Miami, Florida, USA, 8 pages.
<https://doi.org/10.1145/3345768.3355919>

1 INTRODUCTION

The proliferation of networked wireless devices, especially those that populate the Internet of Things (IoT), demands novel approaches for their reliable and efficient interconnection. Relying on RF-based communication alone appears not to be a viable strategy anymore, as the usable RF bandwidth has become limited [3, 20]. In fact, most RF bands—especially those that are license-free—are already no longer efficiently usable due to their limited capacity and to the presence of strong sources of interference. The visible spectrum is a wide and unregulated band that could be effectively used for wireless *Visible Light-based Communication* (VLC). VLC systems could be used in conjunction with traditional RF-based devices to build networks with higher robustness, throughput and spectrum efficiency. Furthermore, as they can be seamlessly integrated with traditional illumination devices, VLC transmitters can be pervasively deployed. As a consequence, hybrid RF/VLC systems can provide an effective solution for the kind of ubiquitous networking required by IoT deployments [1].

Current VLC systems can be broadly categorized into high-end and low-end systems. High-end VLC systems use Field Programmable Gate Array (FPGA) and costly, highly sensitive light sensors [26]. They utilize complex modulation techniques capable to achieve data rates up to Gbps. Most of the high-end systems are meant for infrastructure based deployment, e.g., lighting fixtures as network access points [10]. On the other hand, low-end VLC systems are based on low-cost embedded boards with limited range and data rates [7, 15, 23, 27]. Since these systems have very low bandwidth requirements and mostly operate in narrow, closed spaces, they are ideal to be used in IoT applications, including indoor localization and wireless sensor networking. Our work intends to make a contribution to low-end VLC systems.

In order to keep cost and complexity at bay, low-end VLC systems are based on the commercial-off-the-shelf (COTS) components and embedded boards (e.g., BeagleBone Black) [15, 22, 27]. Light modulation techniques are generally amplitude and pulse-based because of their simplicity. However, they are highly susceptible to ambient noise, i.e., light interference like that from conventional lamps or from sunlight from a window [11, 13, 15, 27]. In fact, one of the major challenges for developing a low-end VLC system is to adopt low-cost design choices that are robust to ambient noise, so that the performance of the system (including BER and data rate) are immune to device placement or illumination.

Several solutions have been proposed to alleviate the problem of ambient noise for low-end VLC systems [4, 6, 8, 28, 29, 31]. Hardware-based approaches focus on intensive analog circuit design, switching Light Emitting Diodes (LEDs) for photodiodes (PD) as receivers or gain control of receiver. Modulation-based approaches adopt frequency-based or other sophisticated modulation techniques. Unfortunately, these approaches suffer from link instability, complex hardware, and high-power consumption. The few prototypes that achieve acceptable robustness to ambient noise have to compromise on range (very short) and data rate (very low).

In this work we contribute to the research on ambient noise-resistant, low-cost, low-power, low-end VLC by designing, developing and testing the VuLCAN (for Visible Light Communication And Networking) system. VuLCAN takes advantage of frequency-based modulation paired with DSP techniques to obtain ambient noise cancellation while maintaining reasonable communication range, data rate and low power consumption. Particularly, VuLCAN employs FSK modulation and adopts the Chirp and Goertzel algorithm for signal detection and demodulation, respectively, thus following a software-defined approach [5, 21]. So far the implementation of such techniques was mainly confined to more high-end DSP boards, FPGA-based platform and costly USRPs. Recent advancements in low-cost high-performance embedded boards, like the ARM Cortex Series boards, afford us the opportunity of bridging the gap between low and high-end systems [19]. Particularly, VuLCAN is based on the ARM cortex-M ST32 F767ZI Nucleo board, which, besides its integrated high-speed Analog-to-Digital (ADC) and Digital-to-Analog Converter (DAC), features native support for operations that are common to DSP techniques.

The contributions of our work are summarized as follows:

- We design, build and test a low-cost and low-power embedded VLC prototype, named VuLCAN, following a software defined approach. VuLCAN achieves a data rate of 65 Kbps over a distance of 4.5 m with low BER (10^{-2}) under varying ambient light conditions (up to 800 lux). We implement the BFSK modulation with a sinusoid as the carrier wave.
- We provide a demodulation scheme based on the use of a Chirp algorithm for signal detection and on the Goertzel algorithm along with Sliding Discrete Fourier Transform (SDFT) for signal demodulation.
- We perform an experimental evaluation to demonstrate the robustness of the system under different indoor scenarios.

The rest of the paper is organized as follows. In Section 2 we describe system design considerations for VuLCAN. Sections 3 and 4 describe the hardware design and the software-defined physical layer of VuLCAN, respectively. Performance evaluation results of the proposed prototype are presented in Section 5. Related works are summarized in Section 6. Finally, Section 7 concludes the paper.

2 SYSTEM DESIGN CONSIDERATIONS

The main focus of our work is to design a system that is robust to ambient noise interference, which can be broadly divided into low frequency (50-60 Hz) and constant additive noise [13, 20]. The former is produced by lights running at the main grid frequency, while the latter mainly comes from natural lighting. This section discusses the system design choices considered for the prototype

implementation. It also provides background information on the modulation, signal detection, synchronization and demodulation techniques chosen.

2.1 Modulation

Binary Frequency Shift Keying (BFSK) is selected as the modulation technique using a sinusoid carrier wave [11]. BFSK, being a frequency modulation approach, offers resiliency to both types of noise identified above. The information transmitted is encoded in the variation of the intensity of the transmitted signal [13]. The instantaneous amplitude of the transmitted wave is proportional to:

$$A(t) \propto \sin(2\pi f(B(t))t + \phi)$$

$$f(s) = \begin{cases} f_0 & \text{if } s = 0 \\ f_1 & \text{if } s = 1, \end{cases}$$

where $f(s)$ is the frequency for symbol s and $B(t)$ is the symbol being modulated at time t and ϕ is the starting phase of the signal. The starting phase can be adjusted in order to have the transmitter power return to 0 after transmitting a symbol. Both symbols have a fixed, equal duration T_s . The bit encoding for our prototype¹ is shown in Figure 1. The duration of the symbol as well as the frequencies can be adapted depending on the ambient noise.

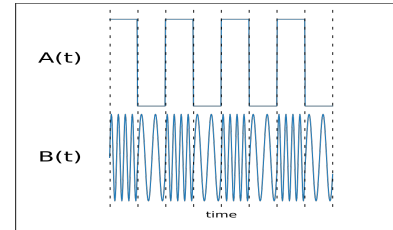


Figure 1: Bit Encoding.

2.2 Demodulation

The recovery of the digital signal from the modulated wave is comprised of two phases: signal detection and demodulation. The receiver produces a stream of values S by sampling the signal at a fixed rate. Standard DSP techniques are then used to identify and extract the frame from the stream.

2.2.1 Signal Detection. Signal detection is performed by pre-pending a chirp to the modulated data. A chirp is a linear sweep signal of finite duration between two frequencies that is represented as:

$$A(t) = A_{max} \sin\left(2\pi\left(\frac{t}{2T}(f_1 - f_0) + f_0\right)t + \phi\right)$$

with $0 \leq t \leq T \wedge f_1 \geq f_0 \geq 0,$

where T is the duration of the chirp, f_0 and f_1 are the starting and final frequencies, A_{max} is the maximum amplitude of the wave and ϕ is the starting phase of the signal [2, 14]. The receiver precomputes the chirp by generating and sampling it at the same frequency as

¹To ensure robust decoding, two periods per waveform are considered for each symbol.

the actual signal. This will constitute the template chirp c_k , the vector of the precomputed values of the chirp of length k . The chirp is detected by performing the correlation of c_k with the values of the stream. Given the stream S , let us call $S_i : S_{i+k}$ the vector of k values of S , starting from i , and also let s_c be the index of the first value of the chirp vector in S , then

$$f(i, k) := (S_i : S_{i+k}) \cdot c_k$$

$$\arg \max_i f(i, k) = s_c \quad \forall k,$$

that is since $f(i, k)$ is the dot product of a slice of the signal with the template chirp it will trivially have its maximum when the signal aligns with the template c_k .

2.2.2 Signal Demodulation. The demodulation is performed by repeated application of Goertzel algorithm to the signal values [21]. This algorithm calculates a single term of the Discrete Fourier Transform (DFT) in time $O(n)$. To recover an individual symbol the terms corresponding to f_0 and f_1 need to be computed and compared. Since the sampling rate of the receiver is R , then the window size, i.e., the number of samples per symbol will be $w_s = \lfloor \frac{T_s}{R} \rfloor$. This constitutes the length of the input that will be fed to Goertzel algorithm at each iteration. It follows that, in order to work, the demodulation window must be at every time aligned with a symbol in the stream. Let $s_d = (s_c + k)$ be the index of the first value of the data in S . If $\frac{T_s}{R} \in \mathbb{Z}$ then the decoding would be trivial since the start of each symbol would always be w_s samples away from the last. However most often $\frac{T_s}{R} \notin \mathbb{Z}$, thus a technique is needed in order to adjust for slight variations in the index of the first sample of the next symbol. This is achieved by using the Sliding Discrete Fourier Transform (SDFT) algorithm [9]. It follows from the definition of DFT that if the value of a term for a window $S_i : S_{i+k}$ of values is known, then the cost to compute the same term for the window $S_{i+1} : S_{i+1+k}$ is in $O(1)$. Consider a symbol with its first sample at index s_d , w.l.g. let it be the symbol for 0, call

$$m_0 = |G((S_{s_d} : S_{s_d+k}), \text{bin}(0))|$$

$$m'_0 = |G((S_{s_d+1} : S_{s_d+k+1}), \text{bin}(0))|,$$

where $G(\text{values}, \text{bin})$ is the Goertzel function, $\text{bin}(s)$ is the bin corresponding to the symbol frequency, and m_0, m'_0 are the magnitudes of the returned vectors. If $m_0 \geq m'_0$ then the window is synchronized with the symbols, otherwise it needs to be adjusted. In this case the next symbol will be decoded starting from $s_d + 1 + w_s$. This whole procedure is repeated L times for a frame of L symbols, thus the complexity of the decoding is linear w.r.t. the length of the frame.

3 HARDWARE DESIGN

The analog hardware design of the transceiver is fundamentally influenced by the chosen modulation technique. The transmission frequencies are constrained by the switching time of the LED, the response time of the PD and the overall bandwidth support of the analog circuitry. Furthermore, additional constraints are imposed by the receiver characteristics such as the ADC sampling rate as well as the processing power available for demodulation. A scheme

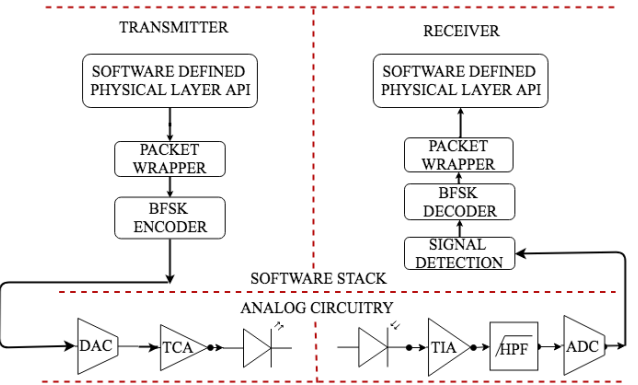


Figure 2: System Architecture.

of the system architecture is shown in Figure 2. The embedded board selected is a low cost STM32-F767ZI Nucleo with integrated high speed ADC and DAC [19]. It is powered by an ARM Cortex-M7 processor, which is especially designed for high performance energy efficient applications. This CPU has a dedicated Floating Point Unit (FPU) as well as a Direct Memory Access (DMA) controller. The DMA in particular completely offloads the CPU from moving the signal data from memory to DAC (for transmission) and from ADC to memory (for reception), as shown in Figure 3. This way it is possible to dedicate more computational power to the actual processing of the signal, which in turn translates into higher data rates. The analog part of the circuitry has been realized using low

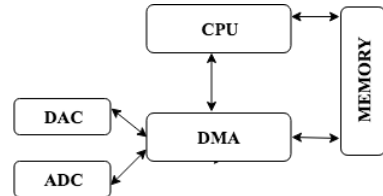


Figure 3: Input/Output Offloading.

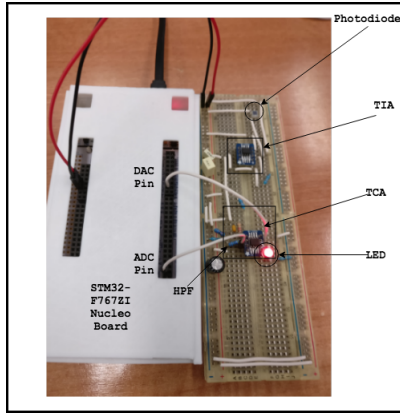
cost COTS components. The approximate cost of our VLC prototype including the prototyping board and the analog circuitry is around 38 euros. The hardware prototype and the list of components are shown in Figure 4 and Table 1, respectively.

3.1 VLC Transmitter

The VLC transmitter (TX) consists of two parts: the Transconductance Amplifier (TCA) and the LED [13]. The TCA converts the voltage from the DAC to the current required to drive the LED, which in turn controls its intensity, and thus the instantaneous amplitude of the wave. The TCA has been selected based on its gain bandwidth product, slew rate, low noise and power consumption. The OPA2301AID has 150 MHz of unity-gain bandwidth and has an available shutdown function that reduces supply current to 5 μ A when not in use is quite suitable for low-power applications. The LED has been selected based on its low power consumption, high directionality and fast switching time. The switching time of

Table 1: Electronic Components Used for the Prototype.

COMPONENT NAME	PURPOSE	PRICE (€)
STM32-F767ZI NUCLEO BOARD	Prototyping Board	€ 23
MTE7063NK2-UR	LED	€ 6
BPW34	Photodiode	€ 1
OPA380AID	Transimpedance amplifier (TIA)	€ 5
OPA2301AID	For Transconductance amplifier (TCA) and High pass filter (HPF)	€ 3

**Figure 4: VuLCAN Prototype.**

the LED determines the maximum transmission rate. The LED has a peak emission wavelength of 630 nm (red) and a field of view (FOV)² of 5°.

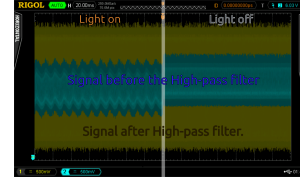
3.2 VLC Receiver

The VLC receiver (RX) consists of a Photodiode (PD), a Transimpedance Amplifier (TIA) and a High Pass Filter (HPF) as shown in Figure 2. The PD used for the prototype is BPW-34, which has been selected based on its fast response time, high surface area (7 mm²) and good sensitivity in indoor applications. The PD is operated in photo-conductive mode, since it provides a better frequency response compared to the photo-voltaic mode. The current flowing through the PD is linearly dependent on the irradiance measured at the surface of the PD. A TIA is used to convert this current to voltage. OPA-380 is selected as the TIA as it provides high slew rate and 90 MHz Gain Bandwidth (GBW). It is ideally suited for high-speed photodiode applications. The gain of the TIA and hence in turn the feedback resistor value has to be accurately chosen which ultimately determines the saturation limit of the VLC receiver. A high gain will give high sensitivity and thus better range, but at the same time will lead to the saturation of the TIA in high ambient light conditions. Whereas a lower gain value is more resilient to external ambient noise but will impair the reception at longer ranges³. The HPF is the last stage of the analog circuit and thus

²Given that the PD has a wide FOV of 65°, by using multiple LEDs or wide FOV LEDs, the omnidirectional communication is possible and hence the prototype is not limited to point to point communication.

³A feedback resistor value of 150K ohms is chosen empirically which achieves best tradeoff in our current settings.

its output is fed to the ADC of the Nucleo STM32-F767ZI board. An active HPF is implemented using OPA2301AID. The choice of the cutoff frequency of the filter is influenced by the transmission and noise frequency. A high cutoff frequency will remove the ambient light noise from artificial luminaries and sunlight as shown in Figure 5. However, there must be a guard band between the cutoff and the transmission frequencies to ensure that the transmission frequencies will not get filtered out.

**Figure 5: Effect of High Pass Filter on Ambient Light.**

4 PHYSICAL SOFTWARE DEFINED LAYER

This section explains the software implementation for data encoding and modulation at the transmitter side, and signal detection and decoding at the receiver side. The firmware is implemented in C language using the HAL library provided by ST-Microelectronics and CMSIS library provided by ARM. These libraries in particular, have been optimized to make use of available FPUs to carry out common DSP operations in an efficient way.

4.1 Firmware for Transmitter

The Software Defined Physical Layer exposes an API to the upper layer of the network stack to queue data for transmission as shown in Figure 2. When a packet gets popped from the queue, it becomes the payload for a physical frame, whose format is shown in Figure 6. The packet wrapper builds the physical frame by pre-pending a preamble to the data. The preamble consists of a chirp followed by two bytes of synchronization (SYNC) bits. The transmitter pre-generates, samples and stores the waveform encoding of every possible byte. A frame to be transmitted is composed by copying the preamble and the byte waveforms onto a memory buffer. The DMA unit is initialized to transfer the values from this buffer to the

Chirp Encoding	Sync Bits	Payload
8 Symbol Periods	2 Bytes	1...64 Bytes

Figure 6: Packet Frame Format

DAC. The rate at which the DAC consumes the buffer determines the transmitting frequency of the signal. The pseudo code of the transmission firmware is shown in Figure 7.

```

def build_frame(packet):
    frame.preamble = fixed_preamble
    frame.payload = packet.data
    return frame

def modulate(frame):
    wave.chirp = generate_chirp()
    for bit in bin(frame):
        wave_symbol = modulate_bit(bit)
        wave.data.append(wave_symbol)
    return wave

def transmit(wave):
    # Start the transfer from memory
    # to DAC unit, returns immediately
    dma_unit.mem_to_dac(wave)

def transmission_done():
    transmitter_cond.signal()

    while True:
        packet = packet_queue.pop()
        frame = build_frame(packet)
        wave = modulate(frame)

        transmitter_cond.wait()
        transmit(wave)

```

Figure 7: Pseudo Code of the Firmware for Transmission.

4.2 Firmware for Receiver

The receiver is always listening for incoming packets. The sampling of the signal is done through the combination of the onboard ADC and DMA. When the receiver is initialized, the ADC is started with a sufficiently high sampling rate and resolution (2.45 MSps and 8 bit, respectively) to ensure the best tradeoff between the conversion rate and the quantization error. The DMA is also started, to copy the values from the ADC to a memory location (logically a circular buffer). The raw data collected from the ADC is shown in Figure 8. This constitutes the stream of values on which the CPU operates to detect and decode the frames. Every time a frame arrives and is decoded, it is put on the outgoing queue from which the upper layer can read. The pseudo code for the receiver firmware is shown in Figure 9.

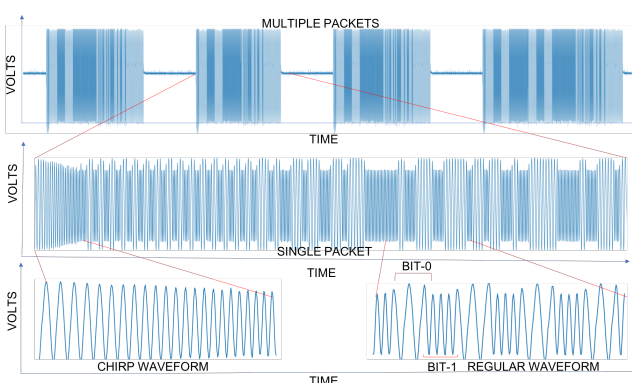


Figure 8: Raw Data Collected from ADC.

```

# Start the DMA unit to copy data
# from the ADC to the memory
dma_unit.adc_to_mem(circ_buffer)

while True:
    # Detect the signal start using the
    # chirp present in the preamble
    signal_start = detect_signal_start()

    # Use the preamble to correct sync
    # errors and find the start of data
    # symbols
    data_start = sync()

    while i < data_len:
        next_bit = decode_symbol(
            data_start + i)
        data.append(next_bit)
        i += symbol_len

    if detect_desync():
        resync()

    frame_queue.push(data)

```

Figure 9: Pseudo Code of the Firmware for Reception.

5 EXPERIMENTAL EVALUATION

We evaluate the performance of our prototype based on the following metrics : Bit Error Rate (BER) vs. Noise floor, BER vs. Distance, Estimated Signal-to-Noise-Ratio (SNR) vs. Distance, Power Consumption and Data Rate. We use a single TX-RX pair for the experiments. All results have been obtained by averaging the outcomes of 1536 packet transmission. This number of packets obtains a 95% confidence with 5% precision. The frame payloads are fixed to 8 and 16 Bytes for the experiments⁴. The experiments are repeated in various indoor scenarios covering different lighting conditions. The illuminance under each condition is measured using the ILM-01-RSPro light meter. The experimental setup is shown in Figure 10. The carrier wave frequencies used for the tests are 130 KHz and 260 KHz for the symbol 0 and 1, respectively. The sampling frequency of the ADC is set to 2.45 MSps which satisfies the Nyquist sampling criteria to ensure synchronization, correct decoding and minimal drifting with higher payloads, given the selected transmission frequencies. The cutoff frequency of the HPF is set to 80 KHz, providing an ample guard band of 50 KHz to the signal. The size of the chirp has been fixed to 114 samples per packet, which provides good signal detection performance while still being relatively fast to compute.

5.1 BER vs. Noise floor

To understand the impact of ambient light on BER, we fix the distance between TX and RX to 1 m⁵ and the frame payload to 8 and 16 Bytes. We have attempted to cover the whole ambient light range possible in indoor scenarios (0-1000 lux). The experiments are performed in indoor scenarios ranging from dark room to room with bright artificial lights and with open and closed windows during daytime. The BER is calculated by comparing the transmitted sequence of bits to the received bits per packet and counting the number of errors. Figure 11a shows that the BER on an average is

⁴It was observed during experiments that the signal decoding algorithm is susceptible to misalignments in the decoding window for higher payloads (54 Bytes onward), leading to higher BER which can be improved by using a forward error correction (FEC) codes.

⁵ We have performed this experiment keeping the distance fixed, well below the maximum range, while the noise floor varies. The distance must remain constant to rule out its impact on the bit error rate.

**Figure 10: Experimental Setup.**

less than 2.71% for the noise floor conditions until 700 lux. Then there is a slight increase in BER and reaches to 5.28% at 800 lux noise floor. Beyond 800 lux, the ambient light saturates the amplifier at the receiver side and hence make it difficult to detect and decode the signals. With our current setup, the VuLCAN works well until 800 lux which spans the entire indoor deployment. It is possible to upgrade the VuLCAN for outdoor deployments by adding highly sensitive light sensors.

5.2 BER vs. Distance

In this scenario, we fix the packet size to 8 and 16 Bytes. The tests are carried out in a noisy scenario of 490 lux (indoor office room with artificial lights on). The distance between TX and RX is then varied to evaluate the range performance. In Figure 11b, we observe that the BER on an average is in the order of 10^{-2} upto 4.5 m. Beyond 4.5 m, we consider the error rate to be unacceptable given the reliability requirements. The increase in BER is mainly due to extremely low signal strength at the receiver with large distances. Thus, the maximum operating range attained by VuLCAN is 4.5 m in an indoor environment. It is important to highlight that this long range is obtained with a low power single LED as the TX. It is mainly due to the effective signal detection algorithm (chirp algorithm) that the receiver is able to detect the signal even with low signal strength. Also, the prior knowledge of the receiver about the transmitted frequencies and the DFT based decoding make it possible to achieve reception at larger distances. In the current version, the working distance is 4.5 m, which is sufficient for indoor networking. Meanwhile, it is possible to improve the range and coverage of the VuLCAN by scaling the design with multiple LEDs or high power LEDs at the TX and with more stages of amplifier at the RX.

5.3 SNR evaluation

To understand the link quality of the signal on the VLC channel effectively, the estimated Signal-to-Noise-Ratio (SNR) evaluation has been conducted with an ambient illuminance at 490 lux. The standard definition of SNR is adopted for calculation.

$$\text{SNR}_{\text{dB}} = 20 \log_{10} \left(\frac{A_{\text{signal}}}{A_{\text{noise}}} \right),$$

where A_{signal} is the root mean square (RMS) voltage of signal and A_{noise} is the RMS voltage of the noise respectively. The estimate of the signal amplitude, A_{signal} is obtained from the recorded trace by fitting the already known transmitted signal waveform to the received values. The estimate of the noise, A_{noise} is calculated by subtracting the estimated signal from the recorded value. We observe from the Table 2 that with the frequency based modulation and demodulation technique, the prototype performs well even with extremely low SNR values.

Table 2: Estimated SNR.

Distance (m)	Estimated SNR (dB)
1.0	22.26
1.5	17.84
2.0	13.04
2.5	9.87
3.0	6.82
3.5	4.62
4.0	3.53
4.5	1.36

Table 3: Power Consumption of the Transceiver.

Components	Power Consumption (mW)
Nucleo Board (TX)	450
Nucleo Board (RX)	530 - 610
LED (MTE7063NK2-UR)	68.4
OPA 2301 (TCA and HPF)	59.5
OPA 380 (TIA)	26
Other components(resistor)	108

5.4 Power Consumption

The power consumption of the VuLCAN is measured as a combination of the TX and RX, as shown in Table 3. For each circuit component, we calculate its power by using the equation $P = VI$. The current flowing through the components is measured using a multimeter. The ARM based cortex-M STM32F7 nucleo board used in our prototype is a high performance device. Considering the aggregated power consumption of the TX and RX, the nucleo board consumes the biggest share ($\approx 67\%$). The LED (along with resistor) used in our prototype consumes 176.4 mW power which is nearly 4 times less the power consumption of high power LED (1-2 W) or multiple LEDs used as a transmitter antenna. The remaining analog circuit blocks including TCA, TIA and HPF consumes around 85.5 mW of power.

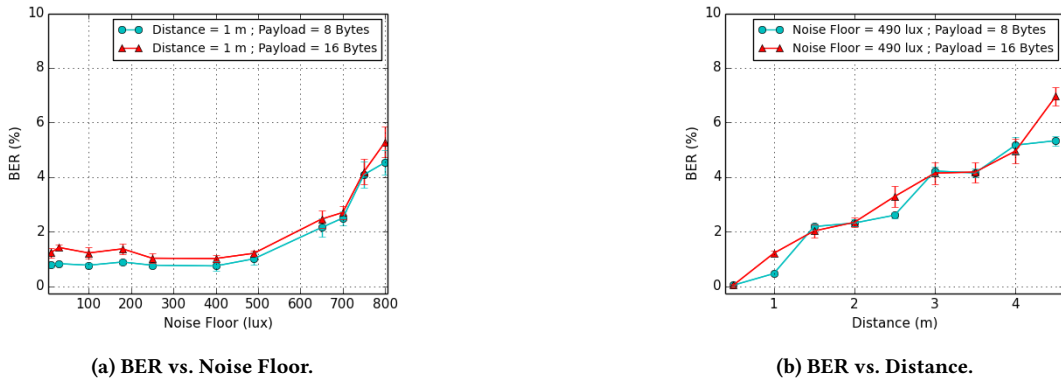


Figure 11: BER as a function of different parameters.

5.5 Data Rate

The data rate of the VLC prototype is mainly determined by the following factors: the ADC sampling frequency, the switching time of the LED circuitry, the slew rate of the OP-AMP, and the response time of the PD. The effective data rate attained by VuLCAN is 65 Kbps which is comparable with the current state of the art prototypes. Such a high data rate makes it suitable for a wide range of IoT scenarios.

6 RELATED WORK

This section aims at providing a brief review of the current state-of-the-art on low-end, embedded VLC prototypes with an emphasis on finding a balance between data rate, range, power and reliability in varied ambient noise conditions.

Schmid et al. present one of the first low-cost LED-to-LED communication system based on pulse position modulation (PPM) achieving a data rate of 800 bps at a distance of 2.5 m [23]. It is unclear if the prototype works in ambient light conditions. OpenVLC 1.0 is the first open source VLC prototype based on an embedded Linux platform (BBB) adopting OOK modulation. It achieves a UDP throughput of 12.5 Kbps at a distance up to 1 m [27]. Heydariaan et al. investigate the performance of the OpenVLC platform under different experimental settings. They report that the maximum ambient light conditions supported by the system is 300 lux [12]. A two-way VLC system with a low power single LED used as both TX and RX is presented in [17]. It achieves a data rate of 3 Kbps at a distance of a few tens of cm. The STM-32 microcontroller is used along with DC-DC booster and 9 W LED in the analog circuit to increase data rate and range performance [18].

Shine is the first low cost VLC platform that demonstrates multi-hop networking [15]. Another interesting work is the proof of concept describing how the Internet Protocol (IP) stack can operate on an LED-based VLC node [22]. However, these works do not report on tests to show resilience to ambient noise conditions. To realize effective VLC networking, robust and stable physical layer solutions are required that take into account the effect of realistic scenarios like ambient light interference.

Zhao et al. took a step forward and proposed a dedicated analog circuit to address the issue of noise cancellation in VLC receivers [31]. Similarly, Chang et al. present an attempt to remove

ambient noise from the VLC circuit [4]. Both works focus on circuit designs without details about data rate and range. Wang et al. present a holistic characterization of the OpenVLC board [28]. Although their approach make the system resilient to noise by utilizing the sensing property of the LED, it shows limited sensitivity and link stability due to switching between PD and LED as the receiver antenna. Schmid et al. present a software-defined adaptive VLC network that adapt the link sensitivity based on the strength of the input signal, obtaining a data rate and range up to 5.50 Kbps and 170 cm, respectively [23, 24]. However, the paper reports the increased uncertainty in the transmission duration and throughput with this approach. Costanzo et al. propose an adaptive VLC system with a fuzzy logic-based process that changes to LEDs of different colors depending on the interfering external lights [6]. The reported data rate was limited to 125 bps at a distance of around 8 m.

In the realm of prototypes addressing the issue of ambient noise cancellation, works worth citing include [8, 16, 25, 29, 30]. An adaptive ambient light cancellation receiver with BFSK modulation has been proposed that is based on OpenVLC platform [29]. The reported operating distance is limited to 50 cm with data rate up to 3 Kbps. *Epsilon* is a VLC prototype for indoor localization. It implements BFSK modulation with channel hopping to avoid collisions of light sources in a shared light medium [16]. Zhao et al. propose a modulation technique encoding data into ultra-short, imperceptible light pulses to sustain communication even when LEDs emit extremely low luminance [25]. The work by Yin et al. concerns a prototype named *Purple VLC* that uses the technique of polarization for bidirectional communication. The reported data rate is 50 Kbps, with a 6 m range in a single link [30]. OpenVLC 1.3 is the third version of the OpenVLC platform with a reported UDP throughput of 400 Kbps at a range of 4 m in noisy conditions [8]. However, a high power LED working at 2.8 W is used for transmission and the upper limit of the noise floor supported by the prototype is not clear.

Table 4 compares our prototype with current state-of-the-art embedded platforms based on their reported performance. When data was not available in the paper we list values based on our estimations based on the described system (items marked with “**”). This birds’ eye comparison clearly shows the advantages of our

Table 4: Comparison of VuLCAN with state-of-the-art related VLC devices.

System Prototype	VuLCAN	Schmid et al. [23]	Klaver et al. [15]	Yin et al. [29]	Yin et al. [30]	Galisteo et al. [8]
Data Rate (Single Link)	65 Kbps	800 bps	1 Kbps	3 Kbps	50 Kbps	400 Kbps
Range	4.5 m	~2 m	~1 m	50 cm	6 m	4 m*
Modulation	BFSK	PPM	OOK	BFSK	OOK	OOK
Implementation	ARM-STM32	Atmel ATmega328P	Arduino	BBB	ARM + PRU	BBB and PRU
Ambient Noise-Floor Limit	800 lux	not reported*	not reported*	400 lux*	[Upper limit not reported]*	[Upper limit not reported]*
Antenna (TX-RX)	LED-to-PD	LED-to-LED	multiple LEDs-to-multiple PDs	LED-to-PD	multiple LEDs-to-PD*	High-Power LED-to-PD
Average Power Consumption	770 mW	~300 mW	4 W*	~315 mA (receiver circuitry)*	not reported*	not reported*

design, and its potential to enhance the RF-based IoT landscape with VLC-based low-cost devices.

7 CONCLUSIONS

We designed, build and tested VuLCAN, an embedded VLC platform for indoor applications that is robust to ambient noise. The prototype is built using the STM32-F767ZI nucleo board and uses low-cost and low-power COTS electronic components. We implemented DSP techniques making use of dedicated hardware and also used I/O offloading for increased efficiency. We evaluated our system under different ambient noise conditions. Results show that it can provide a reliable and robust communication link with low BER and a data rate of up to 65 Kbps over a distance of 4.5 m in the presence of ambient light ranging from 0 to 800 lux. The prototype pushes the envelope of existing low-end embedded VLC design, and expands the range of applications of VLC for IoT.

REFERENCES

- [1] D. A. Basnayaka and H. Haas. 2015. Hybrid RF and VLC Systems: Improving User Data Rate Performance of VLC Systems. In *Proceedings of IEEE VTC*. IEEE, 1–5.
- [2] J.V. Candy. 2016. *CHIRP-Like Signals: Estimation, Detection and Processing A Sequential Model-Based Approach*. Lawrence Livermore National Laboratory, Department of Energy, United States.
- [3] N. Cen, J. Jagannath, S. Moretti, Z. Guan, and T. Melodia. 2019. LANET: Visible-light ad hoc networks. *Ad Hoc Networks* 84 (March 2019), 107–123.
- [4] F. Chang, W. Hu, D. Lee, and C. Yu. 2017. Design and implementation of anti low-frequency noise in visible light communications. In *Proceedings of ICASI*. 1536–1538.
- [5] Cw. Chow, Ch. Yeh, Y. Liu, and Yf. Liu. 2012. Digital signal processing for light emitting diode based visible light communication. *IEEE Photon. Soc. Newsletter* (October 2012), 9–13.
- [6] A. Costanzo, V. Loscri', and S. Costanzo. 2018. Adaptive dual color visible light communication (VLC) system. *Trends and Advances in Information Systems and Technologies* 746 (May 2018), 1478–1487.
- [7] A. Duque, R. Stanica, H. Rivano, and A. Desportes. 2016. Unleashing the power of LED-to-camera communications for IoT devices. In *Proceedings of ACM Workshop on Visible Light Communication Systems*. ACM, 55–60.
- [8] A. Galisteo, D. Juara, and D. Giustiniano. 2019. Research in visible light communication systems with OpenVLC1.3. In *In Proceedings of IEEE WF-IOT*. IEEE.
- [9] R. Garcia-Retegui, S. A. Gonzalez, M. A. Funes, and S. Maestri. 2007. Implementation of a novel synchronization method using Sliding Goertzel DFT. In *Proceedings of IEEE International Symposium on Intelligent Signal Processing*. IEEE, 1–5.
- [10] H. Haas, L. Yin, Y. Wang, and C. Chen. 2016. What is LiFi? *Journal of Lightwave Technology* 34, 6 (March 2016), 1533–1544.
- [11] S. Haykin. 2009. *Communication Systems*. Wiley Publishing.
- [12] M. Heydariaan, S. Yin, O. Gnawali, D. Puccinelli, and D. Giustiniano. 2016. Embedded visible light communication: Link measurements and interpretation. In *Proceedings of EWSN*. Junction Publishing, 341–346.
- [13] S. Hranilovic. 2009. *Wireless Optical Communication Systems*. Springer-Verlag.
- [14] S.M. Kay. 1993. *Fundamentals of statistical signal processing*. Prentice Hall PTR.
- [15] L. Klaver and M. Zuniga. 2015. Shine : A step towards distributed multi-hop visible light communication. In *Proceedings of IEEE MASS*. IEEE, 235–243.
- [16] L. Li, P. Hu, C. Peng, G. Shen, and F. Zhao. 2014. Epsilon: A Visible Light Based Positioning System. In *USENIX Symposium on NSDI*. USENIX Association, 331–343.
- [17] S. Li, A. Pandharipande, and F. M. J. Willem. 2017. Two-way visible light communication and illumination with LEDs. *IEEE Transactions on Communications* 65, 2 (Feb 2017), 740–750.
- [18] C. Liu, X. Jin, W. Zhu, M. Jin, and Z. Xu. 2017. Demonstration of a low complexity ARM-based indoor VLC transceiver under strong interference. In *Proceedings of IWCMC*. IEEE, 622–627.
- [19] ST Microelectronics. 2019. STM32, ARM Cortex- M 7 Nucleo-144 development board. <https://www.st.com/en/evaluation-tools/nucleo-f767zi.html>
- [20] P. H. Pathak, X. Feng, P. Hu, and P. Mohapatra. 2015. Visible Light Communication, Networking, and Sensing: A Survey, Potential and Challenges. *IEEE Communications Surveys Tutorials* 17, 4 (2015), 2047–2077.
- [21] John G. Proakis and Dimitris K. Manolakis. 2006. *Digital Signal Processing*. Prentice-Hall, Inc., NJ, USA.
- [22] S. Schmid, T. Bourchais, S. Mangold, and T.R. Gross. 2015. Linux Light Bulbs: Enabling internet protocol connectivity for light bulb networks. In *Proceedings of the International Workshop on Visible Light Communications Systems*. ACM, 3–8.
- [23] S. Schmid, G. Corbellini, S. Mangold, and T.R. Gross. 2013. LED-to-LED visible light communication networks. In *Proceedings of ACM MobiHoc*. ACM, 1–10.
- [24] S. Schmid, B. von Deschwanden, S. Mangold, and T.R. Gross. 2017. Adaptive software-defined visible light communication networks. In *Proceedings of IEEE/ACM IoT*. IEEE, 109–120.
- [25] Z. Tian, K. Wright, and X. Zhou. 2016. The Darklight Rises: Visible light communication in the Dark: Demo. In *In Proceedings of ACM MobiCom*. ACM, New York City, New York, 495–496.
- [26] D. Tsonev, S. Videv, and H. Haas. 2015. Towards a 100 Gb/s visible light wireless access network. *Optics Express* 23, 2 (Jan 2015), 1627–1637.
- [27] Q. Wang, Giustiniano, and D. Puccinelli. 2015. An open source research platform for embedded visible light networking. *IEEE Wireless Communications* 22, 2 (April 2015), 94–100.
- [28] Q. Wang, D. Giustiniano, and M. Zuniga. 2018. In light and in darkness, in motion and in stillness: A reliable and adaptive receiver for the internet of lights. *IEEE Journal on Selected Areas in Communications* 36, 1 (2018), 149–161.
- [29] S. Yin and O. Gnawali. 2016. Towards embedded visible light communication robust to dynamic ambient light. In *Proceedings of IEEE GLOBECOM*. IEEE, 1–6.
- [30] S. Yin, N. Smaoui, M. Heydariaan, and O. Gnawali. 2018. Purple VLC: Accelerating visible light communication in room-area through PRU offloading. In *Proceedings of ACM EWSN*. Madrid, Spain, Madrid, Spain, 67–78.
- [31] Y. Zhao and J. Vongkulbhaisal. 2013. Design of visible light communication receiver for on-off keying modulation by adaptive minimum-voltage cancellation. *Engineering Journal* 17, 4 (June 2013), 125–129.